RC 22160 (99168) 31 August 2001
Materials Science

IBM Research Report

Characterization of PBGA Laminates Attached with Sn-Ag-Cu Pb-Free BGA Solder Balls

W. K. Choi, S. K. Kang, D.-Y. Shih, P. Lauro, D. Henderson*, T. Gosselin*, D. N. Leonard**
IBM Research Division
Thomas J. Watson Research Center
P.O. Box 218
Yorktown Heights, NY 10598

*IBM Microelectronics
Endicott, NY

**IBM Microelectronics
East Fishkill, NY

Research Division
Almaden - Austin - Beijing - Haifa - T. J. Watson - Tokyo - Zurich

Abstract

During soldering and solder reflow process, the surface finish layer on the PCB laminate reacts and dissolves into the molten solder and the formation of intermetallic compounds (IMC, hereafter). This interfacial reaction would significantly influence the mechanical properties of the solder joint. Moreover, in the extreme case, when the solder joint is subjected to multiple reflow cycles, it would exhibit a drastic change in its microstructure and mechanical properties due to interfacial reactions. Hence the choice of a suitable surface finish is crucial to control the interfacial reactions.

In this study, the effects of surface finish layer on the BGA (Ball Grid Array) solder joints have been investigated as a function of the reflow cycle. A Pb-free solder alloy, Sn-3.8Ag-0.7Cu (in wt%) has been employed as the solder ball material. Five types of surface finish combinations including Cu-Cu, Cu-Au/Ni(P), Au/Ni-Au/Ni(P), Au/Pd/Ni(P)-Cu, and Au/Pd/Ni(P)-AuPd/Ni(P) on opposite ends of the BGA balls, have been investigated. IMC growth was measured as a function of reflow cycles for each surface finish combination. It was found that when Cu was used at least on one side, the IMC grew much faster than those having just the Ni layer. The hardness in the BGA solder ball, was affected mainly by the choice of surface finish, not so much by the reflow cycles. The BGA solder joints having a Ni layer on both sides of the BGA balls showed a higher hardness value than that without a Ni layer. The microstructure of the solder joints varied with the number of reflow cycle and a variance of surface finish. The β-Sn dendrite density and its size appear to affect the hardness value. It appears that the characteristics of the BGA solder joints depend to a great deal on the choice of a surface finish layer due to its interfacial reactions with the solder ball.

Introduction

Sn-based alloys have been developed as Pb-free solder candidates to replace the Pb-bearing solders in microelectronic applications [1-3]. According to the report on Pb-free alloys by the National Center for Manufacturing Science, Sn-Cu and Sn-Ag eutectic, and Sn-Ag-Cu ternary systems have been suggested as promising candidates for Pb-free solders [4]. Among these alloys, the Sn-Ag-Cu ternary eutectic system has the lowest melting temperature (217 ^{o}C) and better interfacial properties than the binary alloys. Thus the Sn-Ag-Cu ternary system has so far received the most attention [3].

The ternary eutectic reaction of the Sn-Ag-Cu system occurs in the composition range of 3.5~4.7 wt.% Ag and 0.9~1.7 wt.% Cu at 217±0.2^{o}C [5-7]. This alloy shows both good solderability and good mechanical properties [8-9]. However, this ternary eutectic temperature is still higher than the Sn-Pb eutectic temperature (183^{o}C), and its composition has much more Sn compared with the Sn-Pb eutectic solder. As a result, it is expected to cause an excessive reaction and growth of IMC during solder reflow [12] and aging processes. To control the interfacial reactions, various types of surface finish layers have been introduced on top of the Cu pad [10-12]. For example, an electroless Ni layer was plated on Cu to reduce Cu dissolution and IMC formation, an immersion Au layer is plated over Ni to prevent surface oxidation. When the Pb-bearing solders were introduced, an optimal surface finish layer must be studied together with their reliability data, because the surface finish layer plays an important role in determining the characteristics of the solder joints, such as their microstructure, interfacial phenomena and mechanical properties.

In the manufacturing assembly processes, multiple reflows are often required. During these processes, the solder joints are subjected to the repeated melting and solidification. This would affect the characteristics of interfacial reaction and their microstructure, and thereby the joint reliability. It has been reported that the fatigue failure happened in the solder region near the IMC [13-14]. And their failure has been explained by the softening effect of the solder matrix due to the changes in microstructure and its composition [15-16] and the stress concentration effect near the interface [17].

During reflow cycles, the microstructure of the BGA solder joints can be affected by the interfacial reactions, such as dissolution of surface finish layers, compositional changes, and IMC growth. Especially, for an extended reflow time during multiple reflows, the depletion in the solder matrix of a particular alloying element can take place in the region adjacent to the IMC. But, when the solder matrix is saturated with dissolving atoms, the dissolution rate of the substrate is reduced [18], which makes an insufficient supply of the solute atoms ahead of the IMC. Thus the solder near the interface may have a lower amount of the solute atoms compared to in the middle of the solder joint. And this depletion can change the microstructure and affect the mechanical properties. A detail study to correlate the microstructure and mechanical properties of a solder joint with the composition change as a function of the reflow cycles is needed.

In this study, BGA solder balls made of Sn-3.8Ag-0.7Cu have been employed to assemble the Hurricane modules having five different combinations of surface finishes. The change of solder joint microstructure with surface finish was investigated as a

function of the reflow cycles using a Scanning Electron Microscope (SEM) and an optical microscope (OM). The composition analysis in the solder ball was also carried out to confirm the dissolution and depletion phenomena near the interface using Energy Dispersive X-ray spectroscopy (EDX), Wavelength Dispersive X-ray spectroscopy (WDX) and Micro X-ray Fluorescence (Micro XRF) technique. The microhardness testing was performed to examine the mechanical properties of the solder balls as a function of the surface finish and reflow cycle.

Experimental Procedures

A. Sample Preparation

The bond pads in the Hurricane modules were plated with three different surface finishes, that include Cu/OSP, Ni (4μm)/Au (0.1 μm) and Ni (4μm)/ Pd (0.38μm)/ Au (0.1 μm). All Ni layers were electroless-plated Ni-P, having approximately 8wt% P content. Pd layer was coated by an electroless plating process, while the thin Au layer was formed by an immersion process.

"Hurricane" laminates were assembled by first attaching 0.89mm solder balls having a composition of Sn-3.8wt%Ag-0.7wt%Cu. A "balled" laminate (called B side, hereafter) was, then, attached (soldered) to another opposing laminate (L side, hereafter) as shown in Fig. 1. By pairing all the different surface finishes, five groups of the Hurricane modules were produced with opposing surface finishes of Cu–Cu, Cu–Au/Ni(P), Au/Ni(P)-Au/Ni(P), Au/Pd/Ni(P)-Au/Pd/Ni(P), and Au/Pd/Ni(P)-Cu.

All the parts were reflowed using the same profile with a peak temperature of 260^{o}C. To examine the effect of reflow cycles, the modules were reflowed 1, 6 and 11 times after the solder balling. Thus the balled side, initially balled before joining to an opposing laminate, experienced one more reflow cycle. Table 1 shows the list of all the "Hurricane" laminates investigated in this study

B. Interfacial Reactions

All the reflowed laminate samples were mounted in epoxy resin and cured at room temperature, first cut with a diamond saw and then mechanically polished with a 0.05 μm alumina slurry. The interface was examined with SEM operated at 25 kV. In order to reveal clearly the presence of IMC at the interface, the solder matrix was etched with 10 %HCl solution for 90 s. To determine the elemental composition of an IMC at the interface, quantitative EPMA (Electron Probe Microanalyser) was used. The IMC thickness was measured in the several selected areas in SEM micrographs from each module.

C. Hardness, Microstructure and Composition of Solder Joints

In order to study the effects of the dissolution of the surface finish layers on the BGA solder joints, the microhardness, microstructure and composition of the BGA balls have been examined as a function of reflow cycles. Microhardness tests were performed using 10 gf load on the cross sections of the BGA solder balls. To compare the microhardness

values near the interface with those in the middle of the BGA solder ball, the tests were carried out both at the positions of approximately 150 μm away from the interface on both B side and L side and in the middle of a BGA solder ball. The microstructure of the BGA solder joints was observed by using an optical microscope as a function of surface finish and reflow cycle. To reveal the solder microstructure, the β-Sn matrix was etched out with the solution of HNO_3:HCl:CH_3OH for several seconds.

The composition near the interface was analyzed by EDX and WDS (Wavelength Dispersive Spectroscopy), while the central area was analyzed by the micro XRF technique.

Results

Fig. 2 shows representative SEM micrographs of the interface microstructures from the B and L sides of Sn-3.8Ag-0.7Cu solder with Cu-Cu surface finish reflowed at 260°C. The IMCs of the scallop shape were formed on both sides. In the B side, the IMC layer grew more than in the L side, and some isolated IMCs spalled from the interface were also seen. From the EDS and WDS analysis, these IMCs were identified as a η-Cu_6Sn_5 phase. The rod type IMC out-grown from the interface in the B side was also observed, being identified as the ε-Ag_3Sn phase.

Fig. 3 reveals the interface microstructures in the B and L sides of Sn-3.8Ag-0.7Cu solder with Au/Ni(P)-Cu reflowed at 260°C. In the B (Au/Ni(P)) side, the IMC morphology is quite different from the typical, faceted Ni-Sn IMC morphology. It was formed as a layer

type and did not show a faceted interface between the IMC and the solder. The similar morphology has been reported by Kang et al [10]. They explained that the Cu in the BGA solder might affect the IMC morphology. In the L (Cu) side, the IMC (η-Cu_6Sn_5) grew much thicker than that in the B side although the L side was reflowed only once.

Fig. 4 depicts the interface microstructures with Au/Ni(P)-Au/Ni(P) after the 2/1 reflow at 260^{o}C. IMCs in both sides have similar morphologies. The IMC shows an irregular morphology. In the solder region, there are a few IMCs spalled from the interfaces. This IMC phase was identified as a Ni_3Sn_4 phase. IMC thickness in both sides was much thinner than the other cases having the Cu surface finish at least on one side.

Fig. 5 shows the interface microstructures with Au/Pd/Ni(P)-Cu after the 2/1 reflows at 260^{o}C. The difference in morphology between the IMCs in the B (Au/Pd/Ni(P)) and L (Cu) sides is obvious. In the B (Au/Pd/Ni(P)) side, the IMC at the interface shows a irregular morphology forming a thin layer and its phase was identified as a Ni_3Sn_4 phase. In the L (Cu) side, although this side experienced only one reflow cycle, the IMC layer was much thicker when compared to the B side. The IMC phase was identified as η-Cu_6Sn_5.

Table II summarizes the growth kinetics of the IMCs for each surface finish and as a function of reflow cycle. Fig. 6 shows the plots of the average IMC thickness in both sides as a function of reflow cycle for different surface finishes. The average thickness was calculated using the measured values of the thickest and thinnest IMC from Table II. In all samples, the Cu-Sn IMC in the Cu side tends to grow more than the Ni-Sn IMC

formed in the Au/Ni(P) and Au/Pd/Ni(P) sides. Especially, as shown in Fig. 6(a), the Cu-Sn IMC growth rate of both sides is large. In Fig. 6(b), the IMC in the Cu side is very thick after only one reflow and then did not grow any more. In Fig. 6(d), however, continuous growth of the Cu-Sn IMC in the Cu side can be seen. It seems the difference may be due to the Pd layer. In the Fig. 6(b), Ni can diffuse from the Au/Ni(P) side to involve the IMC formation at the Cu side. In Fig. 6(c) and 6(e) using a Ni layer in both sides, the growth of the Ni-Sn IMC is very small.

Fig. 7 shows the interfacial microstructures of the BGA solder balls after 12/11 reflows. Their composition analysis is summarized in Table III. Fig. 7(a) is the interface of the B side in the Cu - Cu surface finish. Its phase is η-Cu_6Sn_5 phase, which did not change during the multiple reflows. Fig. 7(b) shows the interface in the Cu side of the Au/Ni(P)-Cu surface finish. The morphology is different from that in Fig. 7(a). It seems to be caused by the Ni content. However, the IMC thickness is similar to that in Fig. 7(a). Fig. 7(c) shows the IMC morphology in the Au/Ni(P) side. The morphology is quite different from Fig. 3(a), not a layer or faceted type. From the composition analysis, the IMC was identified as a Cu_6Sn_5 phase containing a few % of Ni. This result was also confirmed with the IMCs of both sides in Au/Ni(P)-Au/Ni(P) surface finish, as shown in Fig. 7(d). It suggests that the Cu of the Sn-Ag-Cu solder alloy contributed to the interfacial reaction. Thus the IMC formed is not a Ni_3Sn_4 phase, but a η-Cu_6Sn_5 phase. This can cause Cu depletion in the solder region near the IMC.

Fig. 8 exhibits the microhardness values measured as a function of reflow cycles for different surface finishes. Each data point represents the average value of 10

measurements on a cross-section of BGA solder joints. The load for indentation was 10 gf. The microhardness of the BGA solder joints is more sensitive to the type of surface finish than to reflow cycles. In the Au/Ni(P)-Cu and Au/Pd/Ni(P)-Cu surface finishes, the microhardness value increases slightly with the reflow cycles, while in other surface finishes, it tends to go down. But the change in the microhardness is very small in general. From Fig. 9, it can be seen that the microhardness in the surface finishes having a Ni layer at least on one side are higher than those in the surface finish without a Ni layer. Thus, it is expected that the dissolution of the surface finish layer has significantly influenced microhardness. If so, the variation of the microhardness and microstructure may happen according to the location of a solder joint, such as near the interfaces or in the middle of the solder. This may explain why the failure during thermal cycling tests occurs near the interface.

In order to know the microhardness variation depending on the location of a solder ball, the hardness tests have been carried out at three locations using 10gf load. Two locations are approximately 150 μm away from each IMC interface, and one location in the middle of a solder ball. The indentation was performed to avoid hitting the IMC. Figure 9 shows the results of the microhardness variations in the Cu-Cu, Au/Ni(P)-Cu and Au/Ni(P)-Au/Ni(P). It is confirmed that the hardness at all three locations shows the higher value as the surface finishes have more Ni layers. In the Cu-Cu surface finish, as the reflow cycle increases, the microhardness near the B and L sides are reduced, but in the middle is almost constant. After 12/11 reflows, the microhardness in both sides goes down below the value in the middle. The microhardness increase in the middle is due to more Cu dissolutions into the BGA solder ball. However, the Cu depletion in the solder region

ahead of the IMC may cause the reduction of the microhardness. In the Au/Ni(P)-Cu surface finish, the microhardness near the Cu side goes up, and those in the middle and near the Au/Ni(P) side show a little increase with more reflows. However the values near the Au/Ni(P) side do not change. The Ni diffused from the other side has apparently affected the hardness near the Cu side. In the Au/Ni(P)-Au/Ni(P) surface finish, the hardness has a tendency to increase as the number of reflow cycles increases.

In order to know the change in the BGA solder microstructure with a variation of the surface finish and reflow cycles, the BGA solder joints were observed using an optical microscope. Figure 10 shows the optical micrographs of the BGA solder balls in the Cu-Cu, the Au/Ni(P)-Cu and the Au/Ni(P)-Au/Ni(P) surface finishes with a function of reflow cycle. The β-Sn matrix is seen as a dendrite structure. The region between the dendrites corresponds to the eutectic microstructure of Sn-Ag-Cu alloy. The equilibrium microstructure of the eutectic Sn-Ag-Cu system has been reported as the η-Cu_6Sn_5 and ε-Ag_3Sn phases are distributed in the β-Sn grains [5]. The microstructural variation observed here may be due to the non-equilibrium nature of the reflow processes employed. The total area of the dendrite region increases when the Ni layers are used in both sides. Thus the density of the β-Sn dendrite is largest in the Au/Ni(P)-Au/Ni(P) surface finish. It seems to be related with Cu and Ni compositions in the BGA solder ball. As the number of reflow cycles increases, the dendrite density is getting lower and its size becomes larger in all samples. Thus, from these observations, the microhardness can be correlated to the density of the dendrite. That is, as the BGA solder has a densely populated dendrite structure, the microhardness becomes higher.

The solder compositions near the interface and in the middle of the solder balls were observed for Cu-Cu, Au/Ni(P)-Cu and Au/Ni(P)-Au/Ni(P) after 12/11 reflows. The solder composition near the IMC was investigated at the locations about 10 μm far from the interface. In the middle of the solder ball, Ni was not selected for an analyzing element because of the instrument limitation. Table IV shows the composition variations near the IMC and in the middle of the solder ball after 12/11 reflows. In all samples, Cu content in the middle was detected as 1.23, 1.24 and 1.28 wt% for 3 surface finishes. These values are more than the equilibrium Cu solubility (0.16 wt%) at room temperature [5]. The Cu contents in Table IV are close to the Cu solubility (1.23 wt%) in the molten Sn-3.5wt% Ag solder alloy at 250^{o}C through the thermodynamic calculation [16]. It seems the BGA solder ball was solidified fast enough for Cu being frozen with the solubility at 250^{o}C.

Discussions

I. Interfacial Reactions

In general, the IMC growth behavior relies on several factors, such as IMC phase, solder composition, surface finish and processing conditions. In the present study, the IMC phase and solder composition were affected by the surface finish during multiple reflows. Thus, the IMC growth shows its dependence on the surface finish in Fig. 6. When the same surface finish is used on both sides, such as Cu-Cu, Au/Ni(P)-Au/Ni(P), and Au/Pd/Ni(P)-Au/Pd/Ni(P), the IMC grew continuously as the reflow cycle increases. The IMC in the surface finishes having a Ni layer grew at a slower rate than in Cu-Cu. For Au/Ni(P)-Cu and Au/Pd/Ni(P)-Cu, the Cu-Sn IMC on the Cu side grew significantly in

thickness only after 2/1 reflows and then did not grow any more. It means that the driving force for the Cu-Sn IMC growth on the Cu side is greater when a Ni layer is used on the other side. However, after the solder ball is saturated with Cu and Ni from both sides after 2/1 reflows, the growth rate is reduced. In contrast, the IMC in Au/Ni(P) and Au/Pd/Ni(P) sides grew continuously with multiple reflows regardless of another side. Therefore, it reveals that the growth behavior of the IMC with multiple reflows is affected by the surface finish of the opposite side.

As the number of reflow cycle increases, the IMC morphology as well as its phase varied except for the Cu-Cu surface finish. In the Cu-Cu, the η-Cu_6Sn_5 phase grew with a scallop shape and the second phase of ε-Cu_3Sn formed between the η-Cu_6Sn_5 layer and Cu as shown in Fig. 7(a). In the Cu side of Au/Ni(P)-Cu, the Cu-Sn IMC contains a little amounts of Ni after 12/11 reflows, and so morphology is quite different from the scallop shape. The irregular shape of the IMC on the Au/Ni(P) side in Fig. 7(b) and 7(c) changed to a similar shape as Fig. 7(b). It is noted that the Ni-Sn IMC changed into a Cu-Sn phase having a little amount of Ni. It is not clear that there was initially a Ni-Sn IMC layer under the Cu-Sn phase. It seems that this Cu-Sn IMC on Au/Ni(P) is formed by the participation of Cu of the solder in the interfacial reaction. And also in Au/Ni(P)-Au/Ni(P), the Cu-Sn IMC containing a little amount of Ni formed. Thus the Cu depletion may happen on the Au/Ni(P) side. While, Ni of the IMC in the Cu side seems to come from the other side. It, therefore, suggests that the surface finish affects significantly the IMC morphology. From the view of the IMC growth and morphology, Au/Pd/Ni(P)-Au/Pd/Ni(P) surface finish seems to be superior to others. Their IMC grows more slowly and its morphology is also stable during multiple reflows. However, it was not proved

how the dissolved Pd would affect the mechanical property of the BGA solder joints.

II. Microstructure and Microhardness of BGA Solder Joints

From the present study, it was demonstrated that the interfacial reactions affect the microstructure and the microhardness of the BGA solder joints. The dissolution of Cu and Ni can change the phase equilibria of the BGA solder, because even a little amount of Ni or Cu addition into the solder raises the liquidus temperature and so the plastic range between the liquidus and the solidus temperatures becomes wider [16]. It induces the microstructure change during reflow by giving enough time for the BGA solder ball to transform to different microstructure. Furthermore, the more amounts of Cu and Ni in the molten solder provide the more nucleation sites for the dendrite β-Sn matrix to form, and so the β-Sn dendrite becomes denser. Thus Au/Ni(P)-Au/Ni(P) has the densest β-Sn dendrite structure in Fig. 10 due to the presence of both Cu and Ni. However, as the reflow cycle goes on, the IMCs can be precipitated out in the solder matrix and then the amounts of Cu and Ni are reduced. Thus the dendrite density becomes smaller because the number of the nucleation sites decreases. Therefore, as the surface finish has less Ni layers and the number of reflow increases, the dendrite density goes down. As a result, the BGA solder microstructure may depend on the interfacial reaction, that is, dissolution of the surface finish.

As the microhardness is related to the microstructure, the hardness increases as the Ni layer is used. It may result from the denser β-Sn dendrite and higher Ni content in the solder. However, the variation with multiple reflows cannot be explained by the microstructure. Both the density of the β-Sn dendrite and the amount of the IMC

precipitation can affect the hardness of solder joints in a complex way. In Au/Ni(P)-Cu, the hardness goes up with reflow, while in Cu-Cu, it goes down, indicating that the microhardness changes with both the surface finish and the multiple reflow cycles.

In Cu-Cu, the microhardness near the IMC is lower than that in the middle of the BGA solder, while, in the others, it is almost constant regardless of position. In Cu-Cu, because there is a Cu depletion zone ahead of the IMC, the microhardness can be low. And in the others, even though there is a Cu depletion zone, Ni seems to harden the BGA solder ball, yielding no changes.

III. Compositional Analysis of BGA Solder Joints

Cu content near the IMC is lower than that in the middle regardless of the surface finish. This happens due to the IMC growth at the interface which depletes Cu in the BGA solder ball. It is confirmed that Cu is depleted near the IMC and, as a consequence, the microhardness shows a lower value near the interface than in the middle after the 12/11 reflows as shown in Fig. 9. In Au/Ni(P)-Au/Ni(P), Ni was detected more at both sides due to a fast solidification process. Even in the Cu side of Au/Ni(P)-Cu, 0.06 wt% Ni was detected. And as noted from Table II, the IMC phase in the Au/Ni(P) side was identified as the Sn-Cu phase. This means that Ni diffused from the Au/Ni side was enough to change the IMC phase at the other side and affected the characteristics of the BGA solder ball. It proves that Ni plays an important role of hardening the BGA solder ball. In addition, it turned out that the density of the β-Sn dendrite increases when more Ni layers are used as a surface finish because the dissolved Ni can provide a nucleation site for the β-Sn dendrite. Thus, it is confirmed that the reaction and dissolution of a surface finish

layer into the molten solder during reflow cycles can change the composition in the solder ball thereby affecting their microstructure and microhardness.

Conclusions

The effects of surface finishes and multiple reflows on the “Hurricane” laminates modules assembled with BGA solder balls of Sn-3.8Ag-0.7Cu were investigated. Five types of the surface finishes, Cu-Cu, Cu-Au/Ni(P), Au/Ni-Au/Ni(P), Au/Pd/Ni(P)-Cu, and Au/Pd/Ni(P)-AuPd/Ni(P) were included with multiple reflows up to 12 cycles. From this study, the following conclusions are drawn;

1. The IMC on Cu side tends to grow fast, while that on Ni side tends to grow slowly. During the reflow, the elements from each side dissolve sufficiently into the molten solder and reach the other side. Thus they affect the IMC formation in the other side with multiple reflows.

2. It was found that the microhardness in the BGA solder joints is mainly affected by the choice of surface finish, not much by reflow cycle. The surface finish composed of more Ni layers shows a higher hardness value than that without a Ni layer. It is caused by the dissolution of Ni into a solder ball during the reflow, which also influences the microstructure and microhardness of the solder joints.

3. The microstructure of the BGA balls changes with reflow cycles. The β-Sn dendrite is coarsened and its density decreases. This microstructure is closely related to the solder composition which is affected by the dissolution of the surface finish layers. Thus the surface finish metal determines the solder composition, which, in turn, affects the

microstructure and in the end changes the microhardness. Therefore, the choice of a suitable surface finish is the most important factor in affecting the characteristics of BGA solder joints which has been investigated in this study.

References

1. S. K. Kang and A. Sarkhel, J. Elec. Materials, Vol.23, p.701 (1994).

2. K. Nimmo, Proc. The IPC Lead-Free Summit, Minneapolis, October (1999).

3. I. E. Anderson, Proc. NEPCON West'96 Conf., Vol. 2, p. 882-7 (1996).

4. NCMS Report 0401RE96, "Lead-Free Solder Project", National Center for Manufacturing Sciences, Ann Arbor, MI: August (1997).

5. K.-W. Moon, W. J. Boettinger, U. R. Kattner, F. S. Biacaniello, and C. A. Handwerker, J. Elec. Materials, Vol. 29, p. 1122 (2000).

6. C. M. Miller, I. E. Anderson, and J. F. Smith, J. Elec. Materials, Vol. 23, p. 595 (1994).

7. M. E. Loomans and M. E. Fine, Metall. Mater. Trans. A, Vol. 31A, p. 1155 (2000).

8. I. Ohnuma, M. Miyashita, K. Anzai, X. J. Liu, H. Ohtani and K. Ishida, J. Elec. Materials, Vol. 29, p. 1137 (2000).

9. S. W. Yoon, C. J. Park, S. H. Hong, J. T. Moon, I. S. Park and H. S. Chun, J. Elec. Materials, Vol. 29, p. 1233 (2000).

10. S. K. Kang, D. Y. Shih, K. Fogel, P. Lauro, M. J. Yim, G. Advocate, M. Griffin, C. Goldsmith, D. W. Henderson, T. Gosselin, D. King, J. Konrad, A. Sarkhel, K. J. Puttlitz, Proc. 51st Elec. Comp. Tech. Conf., p. 448 (2001).

11. J. W. Jang, D. R. Frear, T. Y. Lee and K. N. Tu, J. Appl. Phys., Vol. 88, No. 11, p. 6359 (2000).

12. S. K. Kang, R. S. Rai and S. Purushothaman, J. Elec. Materials, Vol. 25, p. 1113 (1996).

13. D. R. Frear and P. T. Vianco, Metall. Trans. A, Vol. 25A, pp. 1509-1523 (1994).

14. J.-K. Lin, A. D. Silva, D. R. Frear, Y. Guo, J. -W. Jang, L. Li, D. Mitchell, B. Yeung

and C. Zhang, Proc. 51st Elec. Comp. Tech. Conf., p. 455 (2001).

15. R. J. Coyle, P. P. Solan, A. J. Serafino and S. A. Gahr, Proc. 50th Elec. Comp. Tech. Conf., p. 160 (2000).

16. W. K. Choi, Ph. D Thesis, KAIST (2001).

17. B. Vandevelde, E. Beyne, K. Zhang and J. Caers, Proc. 51st Elec. Comp. Tech. Conf., p. 281 (2001).

18. M. Schaefer, W. Laub, R. A. Fournelle and J. Liang, Proceedings of the Design and Reliability of Solders and Solder Interconnects ed. by R. K. Mahidhara, D. R. Frear, S. M. L. Sastry, K. L. Murty, P. K. Liaw and W. L. Winterbottom, TMS, Warrendale, p. 247 (1997).

Table 1

Hurricane Laminates Attached with BGA (Sn-Ag-Cu) Balls

Module #	Surface Finish (side B)	Surface Finish (side L)	Reflow # at 260 ^{o}C
1	**Cu**	**Cu**	2,1
2	**Cu**	**Cu**	7,6
3	**Cu**	**Cu**	12,11
4	**Au**/Ni(P)	**Cu**	2,1
5	**Au**/Ni(P)	**Cu**	7,6
6	**Au**/Ni(P)	**Cu**	12,11
7	**Au**/Ni(P)	**Au**/Ni(P)	2,1
8	**Au**/Ni(P)	**Au**/Ni(P)	7,6
9	**Au**/Ni(P)	**Au**/Ni(P)	12,11
10	Au/**Pd**/Ni(P)	**Cu**	2,1
11	Au/**Pd**/Ni(P)	**Cu**	7,6
12	Au/**Pd**/Ni(P)	**Cu**	12,11
13	Au/**Pd**/Ni(P)	Au/**Pd**/Ni(P)	2,1
14	Au/**Pd**/Ni(P)	Au/**Pd**/Ni(P)	7,6
15	Au/**Pd**/Ni(P)	Au/**Pd**/Ni(P)	12,11

Table II

IMC growth kinetics as a function of surface finish and reflow cycles

Module #	Surface Finish (side B)	IMC Thickness (μm)	Surface Finish (side L)	IMC Thickness (μm)	Reflow # at 260 C
1	Cu	5-7	Cu	4-5	2, 1
2	Cu	7-12	Cu	7-9	7, 6
3	Cu	9-17	Cu	9-15	12, 11
4	Au/Ni(P)	3-4	Cu	10-12	2, 1
5	Au/Ni(P)	7-10	Cu	10-11	7, 6
6	Au/Ni(P)	6-10	Cu	8-12	12, 11
7	Au/Ni(P)	3-4	Au/Ni(P)	3-4	2, 1
8	Au/Ni(P)	4-5	Au/Ni(P)	5-6	7, 6
9	Au/Ni(P)	4-6	Au/Ni(P)	4-6	12, 11
10	Au/Pd/Ni(P)	3-5	Cu	5-7	2, 1
11	Au/Pd/Ni(P)	5-8	Cu	5-8	7, 6
12	Au/Pd/Ni(P)	5-12	Cu	8-10	12, 11
13	Au/Pd/Ni(P)	3-5	Au/Pd/Ni(P)	2-5	2, 1
14	Au/Pd/Ni(P)	5-7	Au/Pd/Ni(P)	3-5	7, 6
15	Au/Pd/Ni(P)	4-6	Au/Pd/Ni(P)	3-5	12, 11

Table III

IMC Compositions as a function of Surface Finish

after 12/11 Reflow Cycles at 260 ^{o}C

Surface Finish	IMC	Sn (wt%)	Ag (wt%)	Cu (wt%)	Ni (wt%)
Cu-Cu	Cu side	63.05	-	39.95	-
Cu-Au/Ni(P)	Cu side	63.93	0.33	35.1	0.64
	Au/Ni(P) side	63.32	0.3	33.7	2.68
Au/Ni(P)-Au/Ni(P)	Au/Ni(P) side	71.39	0.24	25.49	2.88

Table IV

Lists of the IMC Compositions and the Compositions below the IMC and in the middle of the Solder ball for the Cu-Cu, the Cu-Au/Ni(P) and the Au/Ni(P)-Au/Ni(P) surface finishes.

Surface Finish	Site	Sn (wt%)	Ag (wt%)	Cu (wt%)	Ni (wt%)
Cu-Cu	Near the Cu side	97.71	1.34	0.95	
	In the middle	94.81	3.95	1.24	
Cu-Au/Ni(P)	Near the Cu side	96.31	3.03	0.6	0.06
	In the middle	95.17	3.57	1.26	
Au/Ni(P)-Au/Ni(P)	Near the Au/Ni side	95.21	3.87	0.49	0.43
	In the middle	95.12	3.65	1.23	

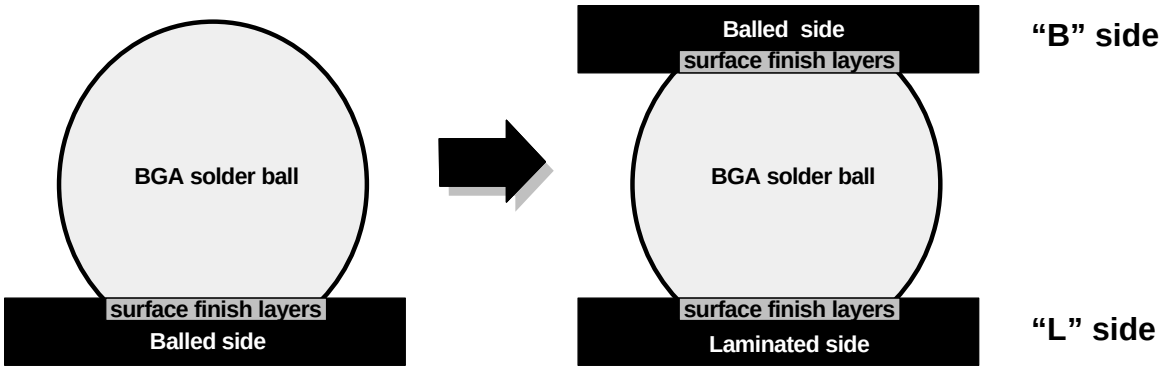

Figure 1 Joining process of PBGA laminates

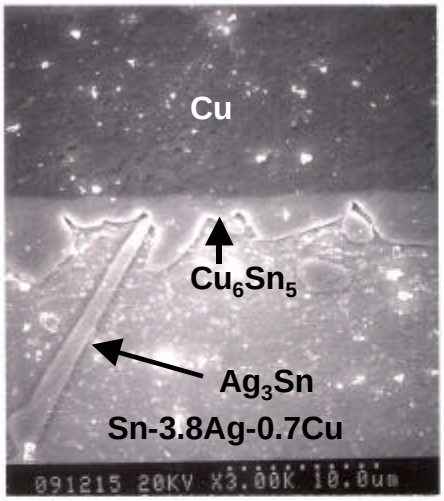

(a) “B” side

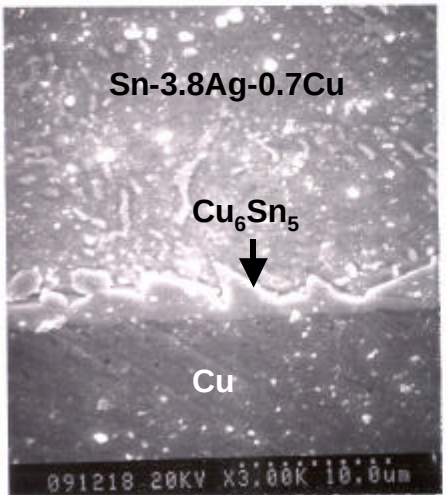

(b) “L” side

Figure 2 Representative SEM micrographs of the interface microstructures of Sn-3.8Ag-0.7Cu solder with the Cu-Cu surface finish after 2/1 reflows at 260^{o}C ; (a) “B” side, (b) “L” side.

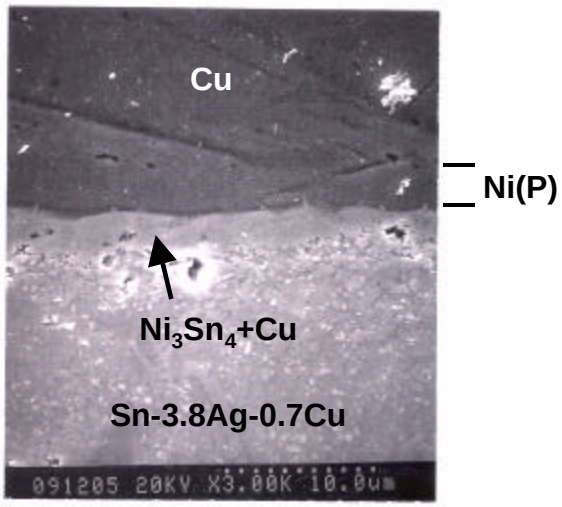

(a) “B” side

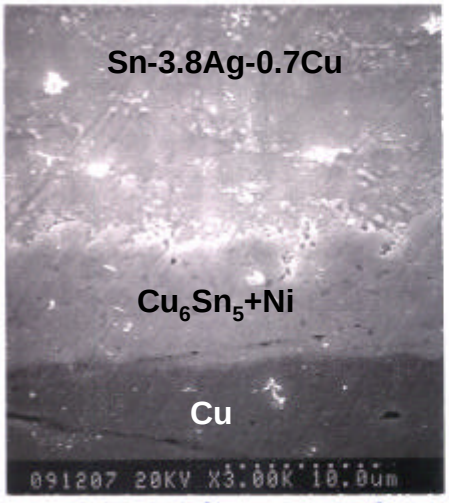

(b) “L” side

Figure 3 Representative SEM micrographs of the interface microstructures of Sn-3.8Ag-0.7Cu solder with the Au/Ni(P)-Cu surface finish after 2/1 reflow at 260°C; (a) “B” side, (b) “L” side.

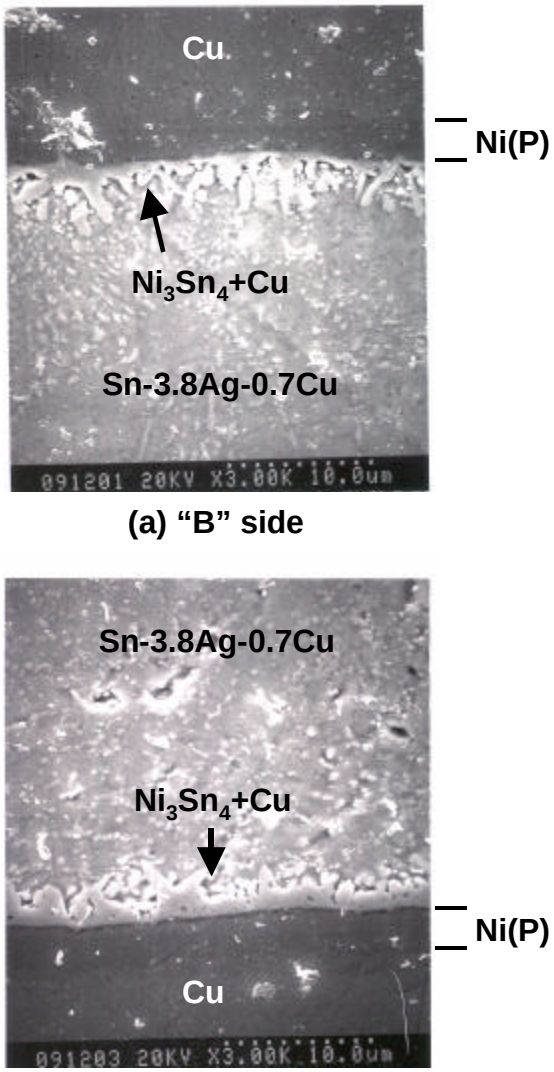

Figure 4 Representative SEM micrographs of the interface microstructures of Sn-3.8Ag-0.7Cu solder with the Au/Ni(P)-Au/Ni(P) surface finish after 2/1 reflows at 260°C ; (a) "B" side, (b) "L" side.

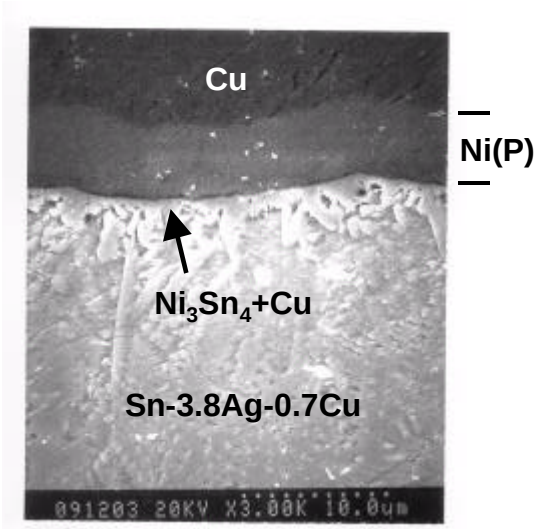

(a) "B" side

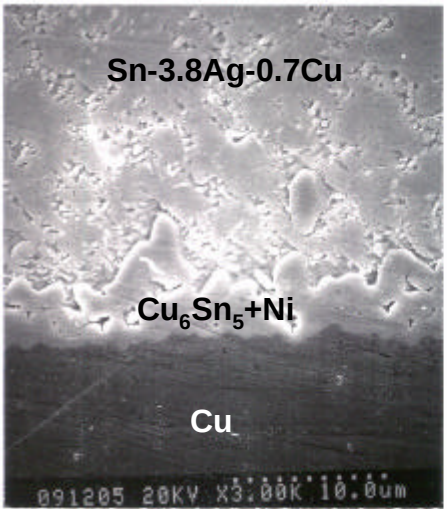

(b) "L" side

Figure 5 Representative SEM micrographs of the interface microstructures of Sn-3.8Ag-0.7Cu solder with the Au/Pd/Ni(P)-Cu surface finish after 2/1 reflows at 260°C; (a) "B" side and (b) "L" side.

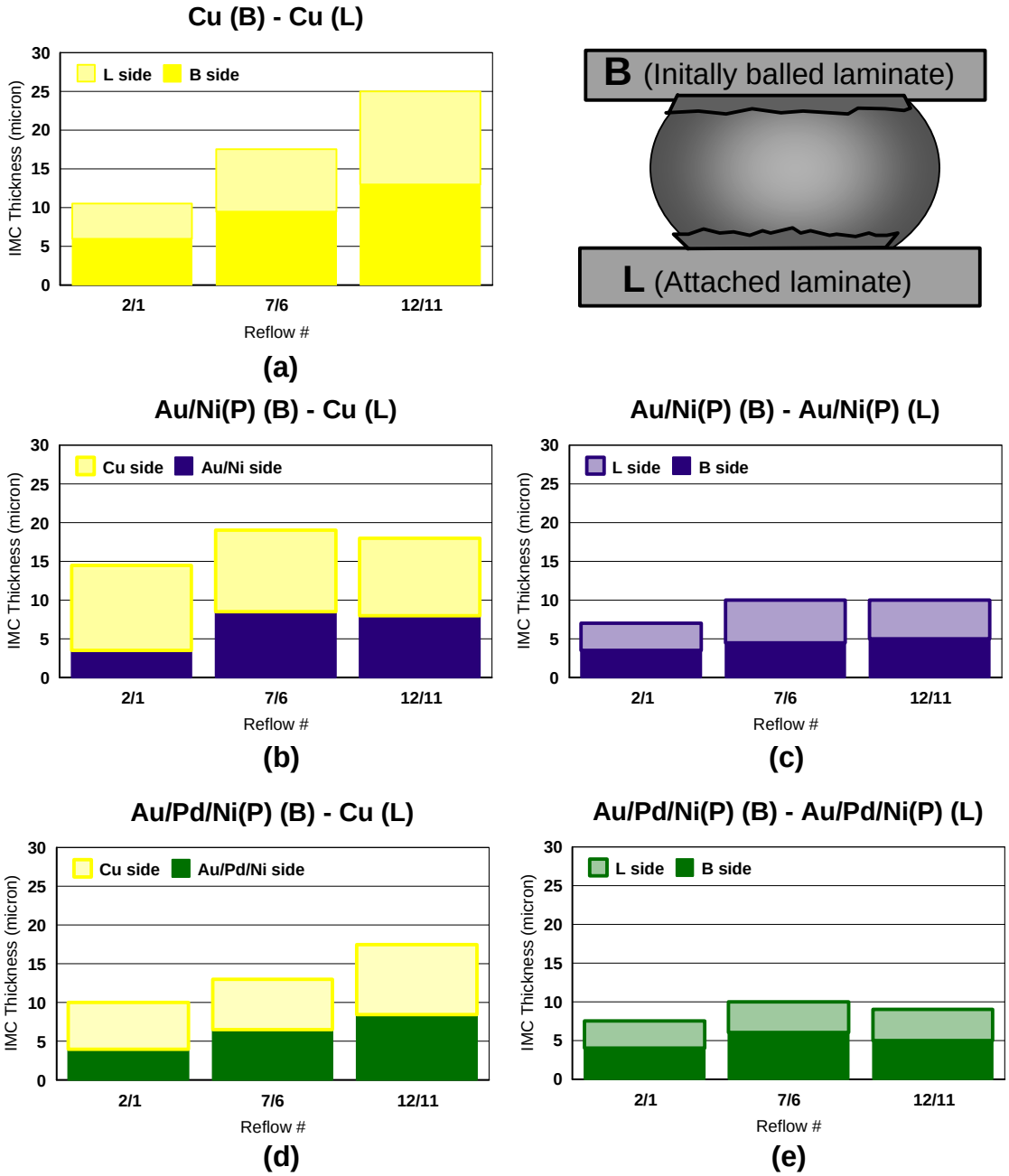

Figure 6 IMC growth kinetics as a function of reflow cycle with different surf ace finishes; (a) Cu-Cu, (b) Au/Ni(P)-Cu, (c) Au/Ni(P)-Au/Ni(P), (d) Au/Pd/Ni(P)-Cu, and (e) Au/Pd/Ni(P)-Au/Pd/Ni(P).

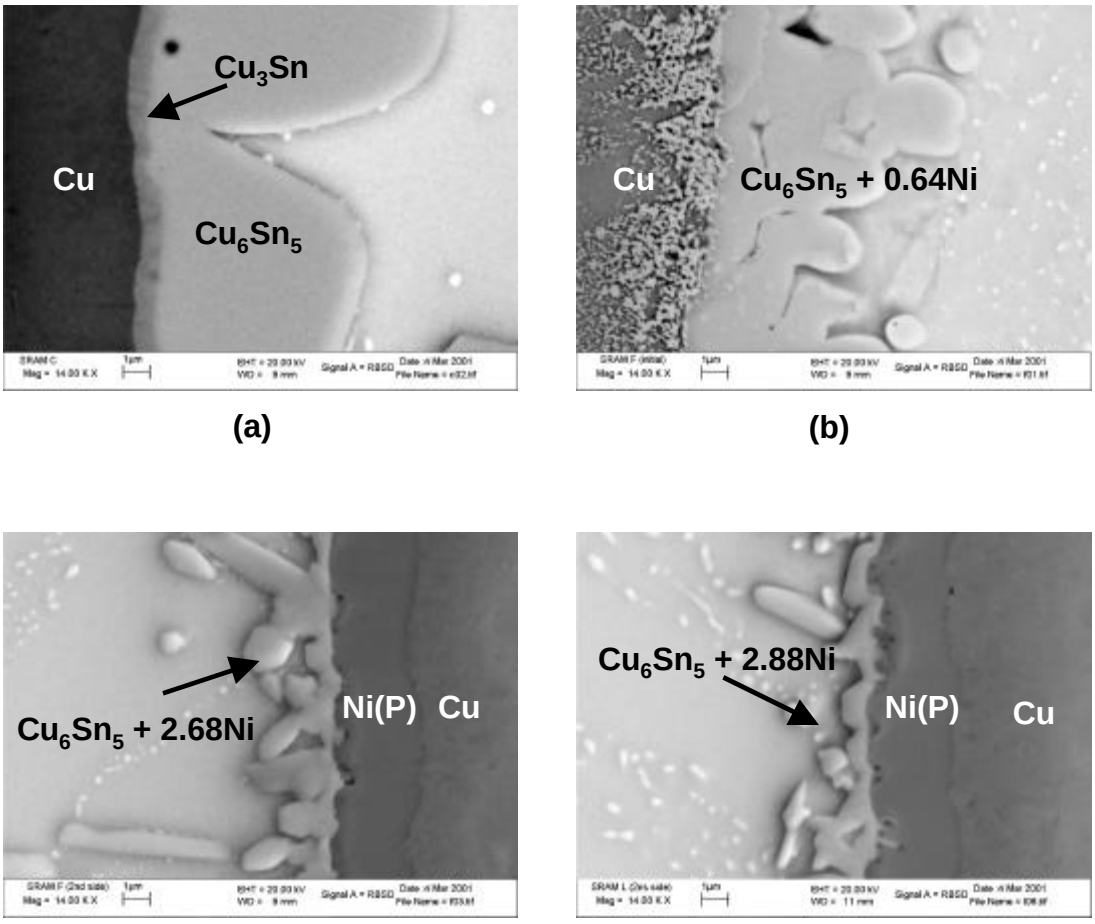

Figure 7 SEM micrographs of the interfacial microstructures of the BGA solder balls after 12/11 reflows : (a) Cu side of Cu-Cu, (b) Cu side of Au/Ni(P)-Cu, (c) Au/Ni(P) side of Au/Ni(P)-Cu,and (d) Au/Ni(P) side of Au/Ni(P)-Au/Ni(P)

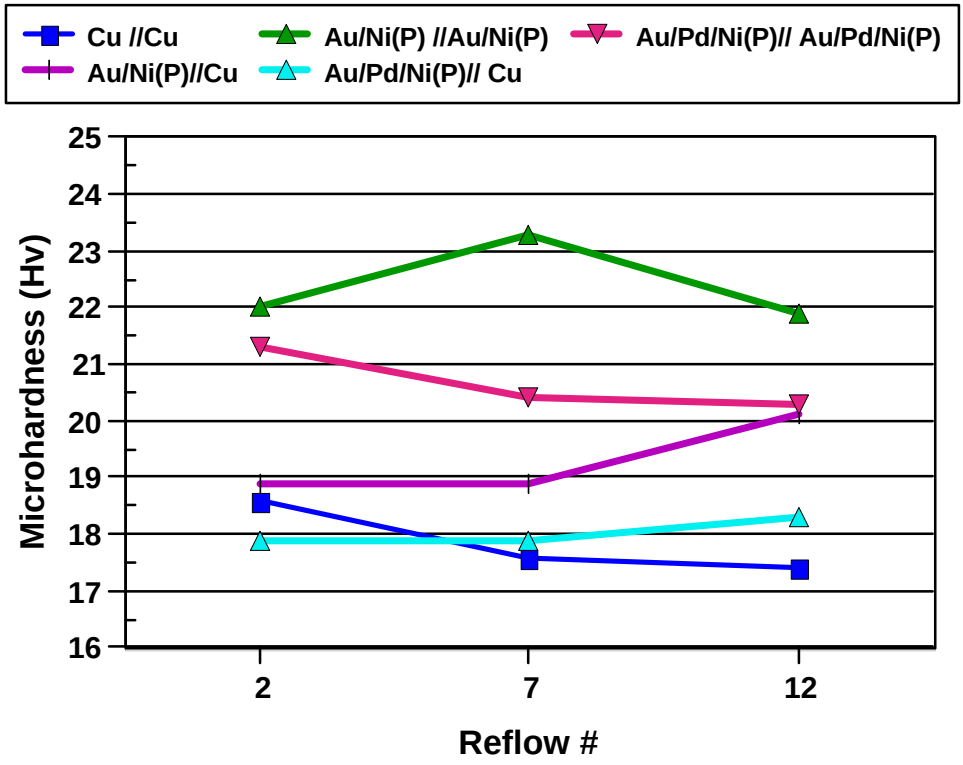

Figure 8 Microhardness variations in the various types of surface finishes as a function of reflow cycle

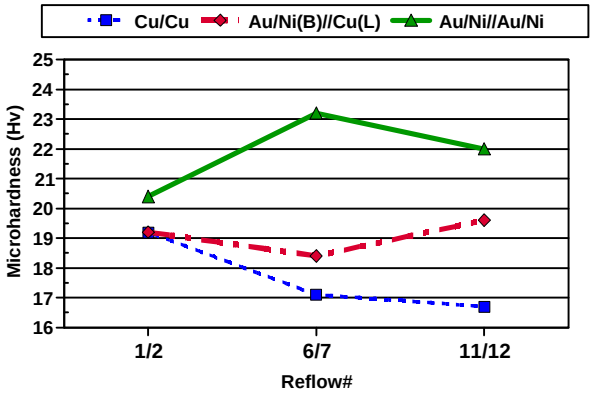

(a)

“B” sidec

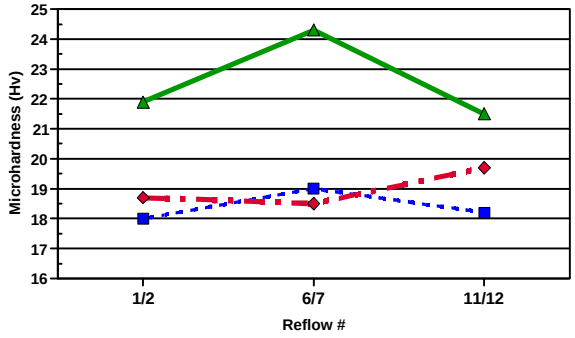

(b)

“Middle”

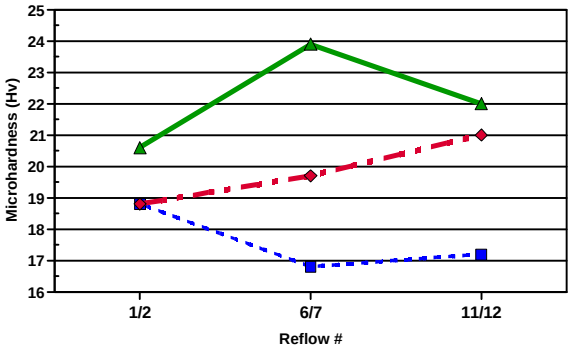

(c)

“L” side

Figure 9 Hardness variations in Cu-Cu, Au/Ni(P)-Cu, and Au/Ni(P)-Au/Ni(P) surface finishes as a function of reflow cycle (a) near B side, (b) in the middle, and (c) near L side.

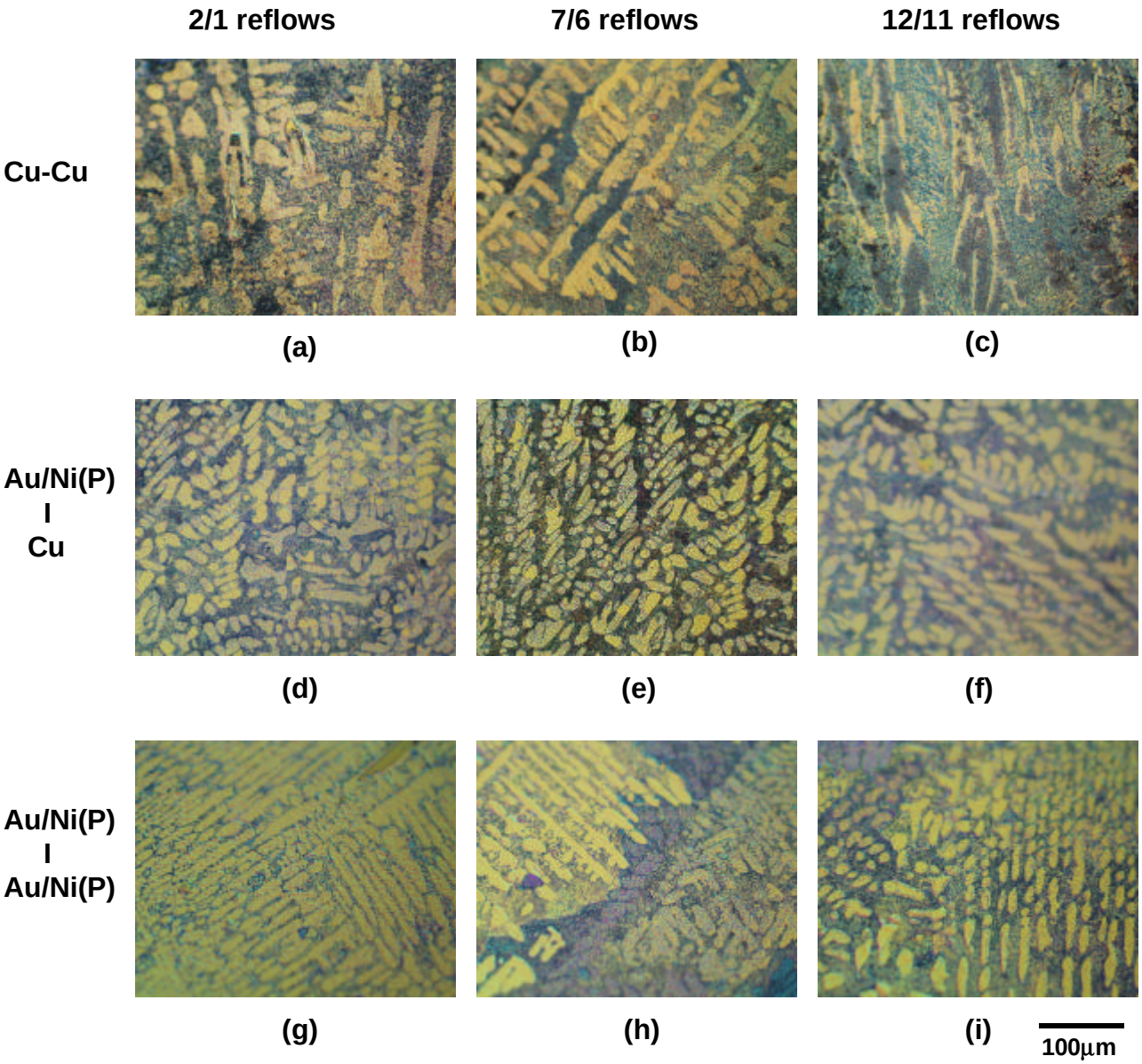

Figure 10 Optical micrographs of the BGA solder balls: (a) after 2/1 reflows, (b) after 7/6 reflows, and (c) after 12/11 reflows in Cu-Cu; (d) after 2/1 reflows, (e) after 7/6 reflows, and (f) after 12/11 reflows in Au/Ni(P)-Cu; (g) after 2/1 reflows, (h) after 7/6 reflows, and (i) after 12/11 reflows in Au/Ni(P)-Au/Ni(P).